

# Compact all-fiber Bessel beam generator based on hollow optical fiber combined with a hybrid polymer fiber lens

Jun Ki Kim,<sup>1</sup> Jongki Kim,<sup>2</sup> Yongmin Jung,<sup>3</sup> Woosung Ha,<sup>2</sup> Yoon Seop Jeong,<sup>2</sup> Sejin Lee,<sup>2</sup> Andreas Tünnermann,<sup>1</sup> and K. Oh<sup>2,\*</sup>

<sup>1</sup>Fraunhofer Institute, Applied Optics and Precision Engineering, Albert Einstein Strasse 7, D-07745 Jena, Germany

<sup>2</sup>Photonic Device Physics Laboratory, Department of Physics, Yonsei University, 134 Shinchon-dong Sudaemoon-gu, Seoul 120-749, South Korea

<sup>3</sup>Optoelectronic Research Centre, University of Southampton Highfield, Southampton SO17 1BJ, United Kingdom

\*Corresponding author: koh@yonsei.ac.kr

Received May 26, 2009; revised August 26, 2009; accepted September 1, 2009; posted September 4, 2009 (Doc. ID 111820); published September 24, 2009

We report a compact all-fiber Bessel beam generator using hollow optical fiber (HOF) and coreless silica fiber based on a self-assembled polymer lens. A nearly diffraction-free Bessel beam pattern was observed with its focused beam diameter of 20  $\mu\text{m}$  maintained over a propagation distance of 550  $\mu\text{m}$ . The generated Bessel beams were experimentally tested under various structural parameters such as the diameters of the HOF and operating wavelengths. A beam propagation method was applied to simulate the proposed device, which shows good agreement with the experimental observations. © 2009 Optical Society of America  
OCIS codes: 050.1940, 060.2310, 140.3300.

Research efforts over Bessel beams have drastically increased, since Durnin *et al.* reported a unique beam shaping technique based on the  $J_0$  Bessel function, theoretically predicting diffraction-free beam propagation [1–3]. In recent years, further investigation efforts over Bessel beams were driven by applications in optical trapping [4] and bioimaging technology [5]. Prior Bessel beam generation techniques have been based on bulk optics such as annular aperture and spherical bulk lens or axicons [6,7]. The main disadvantages of using a bulk optic configuration are their large form, high system cost, and alignment problems. Replacing prior bulk optic components with optical fiber equivalents will provide more flexible and easily deployable instrumentation [8,9]. In this regard, the fiber-optic integration for Bessel beam generation is timely and indispensable.

Here we propose and demonstrate an all-fiber Bessel beam generation technique to axially concatenate hollow optical fiber (HOF) [10], coreless silica fiber (CSF), and a self-assembled polymer lens in a compact package [11], for the first time to the best knowledge of the authors. The HOF was fabricated by a modified chemical-vapor deposition process, and it has a three-layer structure that consists of a central airhole, a germanosilicate ring core, and a silica cladding [10]. In comparison with a fiber axicon lens [9], our method utilizes the original idea of a Bessel beam to form an annular aperture and a spherical lens by HOF and a polymer lens, respectively, to provide a longer nondiffractive propagation distance.

An ideal theoretically diffraction-free Bessel beam would propagate an infinite distance without a change in its beam diameter; its mathematical expression is as follows:

$$\Phi(x, y, z; \kappa) = \exp[i\beta z] J_0(\alpha \rho), \quad (1)$$

where  $\Phi$  is the electric field component propagating in the  $z$  direction,  $x^2 + y^2 = \rho^2$ , and  $J_0$  is the zeroth-

order Bessel function of the first kind.  $\alpha$  and  $\beta$  are the longitudinal and radial wave vectors, with  $\kappa = \sqrt{\alpha^2 + \beta^2} = (2\pi/\lambda)$  ( $\kappa$  is the wave vector and  $\lambda$  is the wavelength) [1–3]. A schematic diagram of the proposed device is shown in Fig. 1. The device consists of serially concatenated HOF, CSF, and a polymer lens tip. In the proposed Bessel beam generator, HOF serves as the annular slit as in [1]. Three different kinds of HOF, characterized by their airhole sizes, were adopted in this study.

Concatenation of HOF to CSF could achieve two unique optical functions. The first is the beam expansion of the HOF ring pattern along the CSF region. The second is to provide the appropriate length between the annular HOF slit and the polymer lens to match the focal length. The ring-shaped beam pattern from the end of HOF will propagate along the CSF region where the ring pattern is expanded to form an appropriate overlap as shown in Fig. 1(a), which will be focused by the self-assembled polymer lens tip for the effective Bessel beam generation.

In theory, the diffraction-free propagation distance of the Bessel beam,  $Z_{\text{max}}$ , depends on focal length  $f$ , the diameter of annular aperture  $d$ , and radius parameter  $R$ , as follows [1,6]:

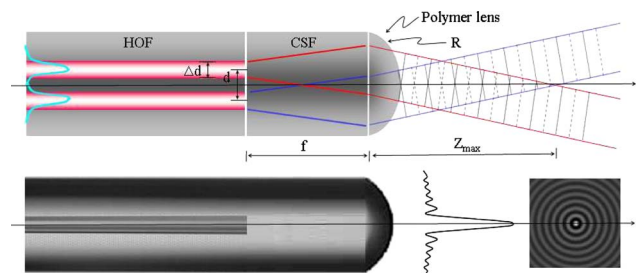


Fig. 1. (Color online) Schematic diagram of all-fiber Bessel beam generator and microscope image of the proposed device serially concatenated HOF, CSF, and polymer lens tip. Inset, expected typical Bessel beam pattern.

$$Z_{\max} \approx \frac{R}{d/2f}, \tag{2}$$

where  $R$  is the smaller radius of the polymer lens or the effective radius of the diffraction pattern:

$$R_{\text{eff}} = \frac{d}{2} + \frac{f\lambda}{\Delta d}. \tag{3}$$

Here  $d$  and  $\Delta d$  are the diameter of the airhole and the width of the ring core of HOF, respectively, and  $\lambda$  is the operating wavelength in vacuum. Based on Eqs. (2) and (3), we can design an all-fiber Bessel beam generator with appropriate design parameters for HOF (the annular aperture), CSF (the beam expander and focal length controller), and a polymer lens (the focusing element). The  $Z_{\max}$  of the proposed structure were estimated as 2100, 1050, and 700  $\mu\text{m}$  in HOF diameters of 10, 20, and 30  $\mu\text{m}$ , respectively.

We numerically analyzed the proposed all-fiber Bessel beam generator using a commercial beam propagation method (BPM) package, BeamPROP. The composite structure (HOF–CSF–lens) was modeled for three different airhole diameters of HOF and the output Bessel beam intensity profiles are depicted in Fig. 2. The HOF airhole diameters were (a) 10, (b) 20, and (c) 30  $\mu\text{m}$ , respectively, and the thickness of the ring core of HOF was fixed at 3  $\mu\text{m}$ . The relative index difference  $\Delta$  between the ring core and the cladding was 0.5%, similar to conventional

single-mode fiber (SMF). The length of CSF was 150  $\mu\text{m}$ , which is the same as the focal length of the polymer lens. The radius of curvature of the polymer lens was 70  $\mu\text{m}$ . Note that it is precisely equivalent to the bulk optics Bessel beam generation technique based on an annular aperture and a spherical bulk lens [6]. As shown in Figs. 2(a)–2(c), we can clearly see the diffraction-free Bessel beam generation over the distance longer than  $\sim 500 \mu\text{m}$ , almost without deformation. It is noteworthy that the number of sidelobes increases along with reduction of the lateral width of the central lobe when the airhole diameter of HOF increases. For a clearer illustration, we also show the beam divergence of the HOF with a 30  $\mu\text{m}$  airhole diameter without CSF and a polymer lens in Fig. 2(d). In comparison with Fig. 2(c), the ring-shaped beam from the end face of HOF in Fig. 2(d) shows Bessel beam effects but quickly diverges into free space with a significant diffraction. Furthermore, the far-field pattern in Fig. 2(c) is a ring-shaped beam, which is more clearly seen in the contour map of the transverse field profiles in Fig. 2(e), as shown in Fig. 2(e). In principle, the far field of the Bessel beam through a lens should be a ring pattern since the Fourier transform of a thin ring is a  $J_0$  function.

For our experiments we used three types of HOF with airhole diameters of 10, 20, and 30  $\mu\text{m}$ . The index difference between the core and the cladding was 0.5% as in conventional SMF. A short length segment of CSF was serially spliced to HOF with appropriate arc conditions to keep the airhole intact. UV curable polymer (Efron WR-346 from Luvantix) was dropped onto the cleaved endface of the CSF to form a lens by surface tension assisted self-assembly. Detailed descriptions of polymer and composition are described elsewhere [11]. The radius of curvature of the fabricated polymer lens and the length of CSF were 70 and 150  $\mu\text{m}$ , respectively.

The measured near fields and mode intensity distributions of the generated Bessel beams for three different kinds of HOF are depicted in Fig. 3. The airhole diameters of HOF are 10, 20, and 30  $\mu\text{m}$ , respectively; the ring core thickness of 3  $\mu\text{m}$  and the outer cladding diameter of 125  $\mu\text{m}$  were used to within 1% tolerance. Note that the mode intensity distributions from the proposed device did show Bessel beam distribution. We also found that the number of sidelobes

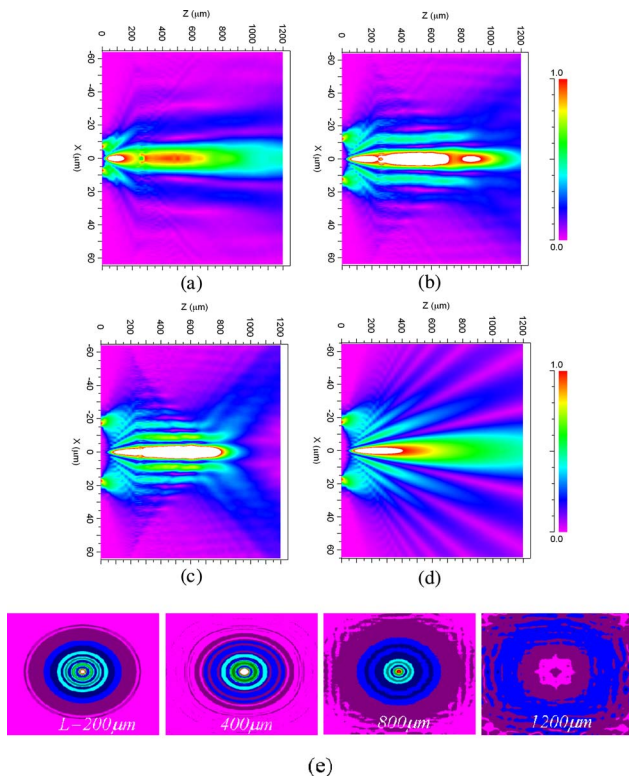


Fig. 2. (Color online) Simulated results of the Bessel beam propagation for the proposed structure using BeamPROP. Top view of the beam intensity in airhole diameters of (a) 10, (b) 20, and (c) 30  $\mu\text{m}$ ; (d) beam diverging properties on the 30  $\mu\text{m}$  airhole without a polymer lens and CSF structure; (e) contour map of the transverse field profiles in (c).

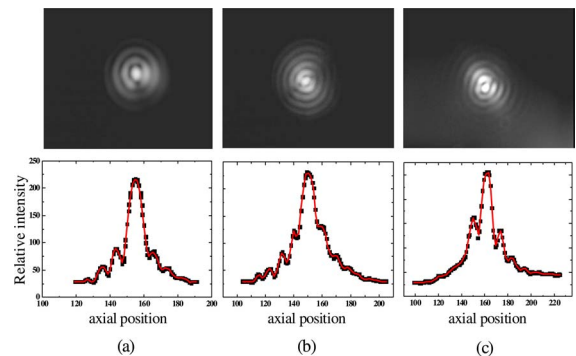


Fig. 3. (Color online) Near-field images of the generated Bessel beam and mode intensity distributions along with different HOF airhole diameters of (a) 10, (b) 20, and (c) 30  $\mu\text{m}$  at a 1550 nm operating wavelength.

increased and the central widths were sharpened as the airhole diameter increased, which is in good agreement with the simulation results shown in Fig. 2.

Beam propagation properties of the fabricated devices on the  $X$ - $Z$  plane were measured by immersing them into a milk-water solution in a microchamber to observe scattering traces in the visible wavelengths. The chamber was mounted on a microscopic glass slide and the beam pattern was observed with a CCD camera and a microscope. Figures 4(a) and 4(b) show the propagation images of the Bessel-like beam from the proposed device and the Gaussian beam from cleaved SMF, respectively, at a 635 nm laser diode wavelength. To compare the two cases clearly, the microscope images were measured without illumination at the back, as shown in Figs. 4(c) and 4(d). The intensity distribution profiles of the images are also depicted in Fig. 4(e). It is noteworthy that the proposed device showed a significantly longer and non-

diffractive propagation length than the normal properties of a Gaussian beam. We could observe a Bessel-like beam propagation from the proposed device over 550  $\mu\text{m}$  without any significant deformations in the case of a 30  $\mu\text{m}$  airhole diameter HOF. The beam drastically diffracts over the propagation length of 680  $\mu\text{m}$ , and the simulation predicted almost 1000  $\mu\text{m}$  as shown in Fig. 2(c).

In summary, we have demonstrated an all-fiber Bessel beam generator by providing a unique compact structure in a serial concatenation of hollow optical fiber, coreless silica fiber, and a polymer lens. We experimentally confirmed that the fabricated device showed a Bessel-like beam propagation without deformation up to 550  $\mu\text{m}$ , which is consistent with a beam propagation method analysis. The compactness and inherent fiber compatibility of the proposed device can have high potential in various optical applications including optical trapping, optical coherence tomography imaging, as well as high precision laser processing.

This research was supported in part by the Korea Science and Engineering Foundation (KOSEF) (programs R01-2006-000-11277-0 and R15-2004-024-00000-0), the Korea Foundation for International Cooperation of Science and Technology (KICOS) (program 2007-8-0536, 2007-8-1864, and 2007-8-1867), the Korea Institute of Industrial Technology Evaluation and Planning (ITEP) (program 2007-8-2074), and the Brain Korea 21 Project of the Ministry of Education.

## References

1. J. Durnin, J. J. Miceli, Jr., and J. H. Eberly, *Phys. Rev. Lett.* **58**, 1499 (1987).
2. J. Durnin, *J. Opt. Soc. Am. A* **4**, 651 (1987).
3. J. Durnin, J. J. Miceli, and J. H. Eberly, *Opt. Lett.* **13**, 79 (1988).
4. D. McGloin, V. Garces-Chavez, and K. Dholakia, *Opt. Lett.* **28**, 657 (2003).
5. Z. Ding, H. Ren, Y. Zhao, J. S. Nelson, and Z. Chen, *Opt. Lett.* **27**, 243 (2002).
6. Y. Lin, W. Seka, J. H. Eberly, H. Huang, and D. L. Brown, *Appl. Opt.* **31**, 2708 (1992).
7. R. M. Herman and T. A. Wiggins, *J. Opt. Soc. Am. A* **8**, 932 (1991).
8. S. Ramachandran and S. Ghalmi, in *Conference on Lasers and Electro-Optics* (Optical Society of America, 2008), paper CPDB5.
9. S. K. Mohanty, K. S. Mohanty, and M. W. Berns, *Opt. Lett.* **33**, 2155 (2008).
10. K. Oh, S. Choi, Y. Jung, and J. W. Lee, *J. Lightwave Technol.* **23**, 524 (2005).
11. J. Kim, M. Han, S. Chang, J. W. Lee, and K. Oh, *IEEE Photon. Technol. Lett.* **16**, 2499 (2005).

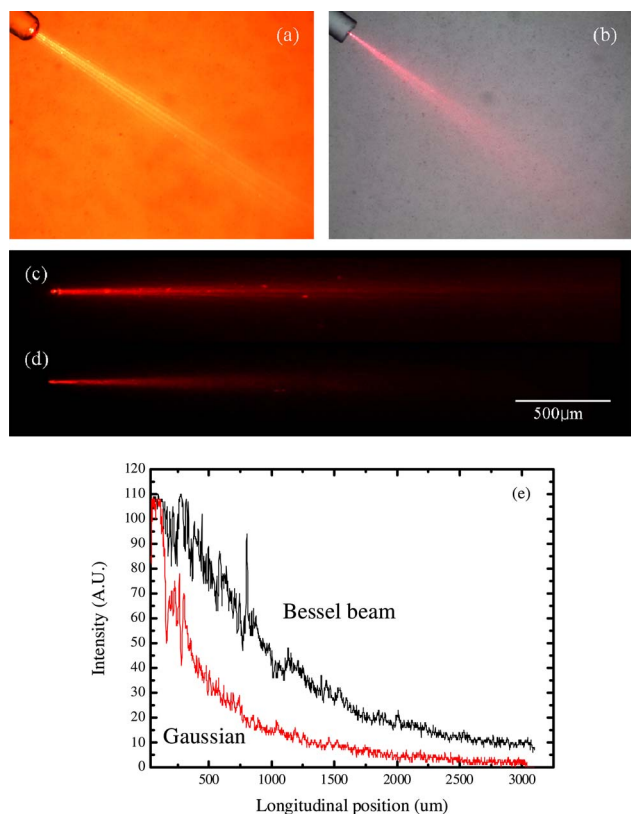


Fig. 4. (Color online) Beam propagation images on the  $X$ - $Z$  plane in a milk-water solution: (a) Bessel beam from the proposed device; (b) Gaussian beam from cleaved SMF at a 635 nm operating wavelength; (c), (d) images of (a) and (b) without microscope illumination at the back, respectively; (e) intensity distribution profile of (c) and (d).